

# Biological Applications of Graphene and Graphene Oxide

Congyu Wu, Yan zhang, Xiaochen Wu, Yongqiang Yang, Xuejiao Zhou, Haixia Wu\*

Key Laboratory for Thin Film and Microfabrication of the Ministry of Education, Research Institute of Micro/Nano Science and Technology, Shanghai Jiao Tong University, Shanghai 200240, P. R. China.

\* Corresponding author: [haixiawu@sjtu.edu.cn](mailto:haixiawu@sjtu.edu.cn)

## Abstract

Graphene, as a steady two dimensional (2D) carbon material, possesses intriguing physical and chemical properties, which arouses great interests of scientists for its applications in enormous fields. In particular, graphene and graphene oxide have been widely used for drug delivery and DNA detection based on  $\pi$ - $\pi$  stacking and hydrophobic interactions. Besides, graphene with fluorescent molecules or nanoparticles and graphene quantum dots have also been frequently applied as fluorescent probe. In this article, advances of graphene and graphene oxide on biomedical applications will be highlighted from the perspective of biomolecular interaction, cell imaging, drug delivery, and toxicity.

**Keywords:** Biological application, Graphene, Graphene oxide, Toxicity

**Citation:** C.Y. Wu et al. Biological applications of Graphene and Graphene Oxide, *Nano Biomed. Eng.* 2012, 4(4), 157-162.

DOI: 10.5101/nbe.v4i4.p157-162.

## 1. Introduction

Graphene, a recently discovered carbon nanomaterial with two-dimensional (2D) atomic layered structure, has been proven to show unique chemical/physical properties. The mechanical exfoliation method is the first approach to graphene from graphite, pristine graphene [1]. After that several alternative approaches including top-down and bottom-up methods, such as arc discharge method [2], chemical vapor depositon (CVD method) [3,4] and chemical reduction of graphene oxide (CRGO) [5-8] have been developed, and the pristine graphene and its derivatives have been produced in large scale.

More and more attention has been attracted to this special 2D graphitic sheet in the past decade, due to its pronounced electrical conductivity, good thermal conductivity and abnormal mechanical flexibility [9-11]. For instance, the novel 2D nanostructure has been intensively implemented to explore potential applications on super-capacitor, batteries, field-effect transistors (FETs), optical sensors and so on [12,13].

However, the lower water-solubility and the irreversible aggregation due to the strong  $\pi$ - $\pi$  stacking hinders the wide application of graphene nanosheets in biomedical field. Using capping reagents (polymers or surfactant), the water solubility and the stability of graphene sheets could be improved dramatically, but in the cost of the biological compatibility. Thus, graphene oxide (GO), one derivative of gaphene, has been used more frequently in

the biological system owing to its relatively higher water solubility and biocompatibility [7,10,14,15]. In this mini-review, the current achievements of graphene and GO on biomedical research are summarized in the view of biomolecular interfacing, cell imaging, drug delivery, and toxicity.

## 2. Biomolecular interfacing

Researches about the effects of graphene sheets and/or GO on macro-biomolecules, such as DNA molecules [16-18], gene [19], and enzymes [20], have caught great interests, where results have shown several potential applications in bioassay and bioanalysis.

Based on the  $\pi$ - $\pi$  stacking between GO and ssDNA, the complexes of GO and single-stranded DNA (ssDNA) have been assembled. As a fluorescence quencher, graphene sheets were used as a platform for sensing DNA (Fig. 1) [21].

It has been demonstrated that the fluorescence of the dye FAM is quenched after the FAM-labeled ssDNA bonded on GO via  $\pi$ - $\pi$  stacking force. Because the hydrogen bond between the FAM-labeled DNA and complementary DNA is stronger than nonspecific binding force between the FAM-labeled ssDNA and GO, the FAM-labeled ssDNA detaches from GO, and the fluorescence could be recovered when complementary DNA molecules added. This general method was also

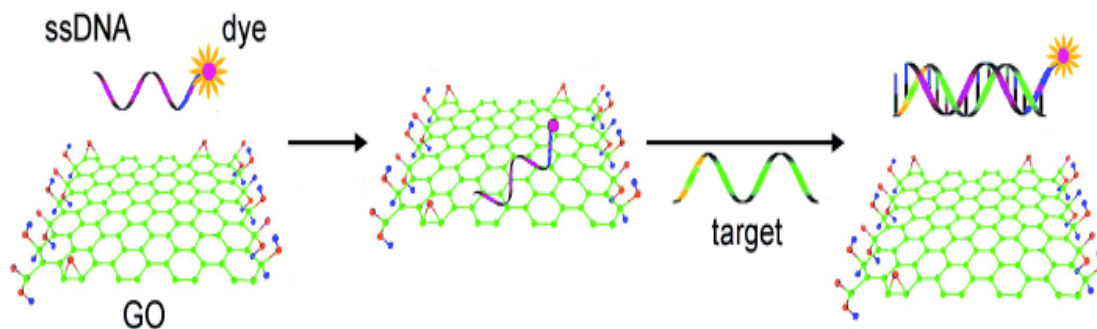


**Fig. 1** Schematic representation of the target-induced fluorescence change of the ssDNA-FAM-GO complex. FAM is the fluorescein-based fluorescent dye. Copyright permission from ref. 21.

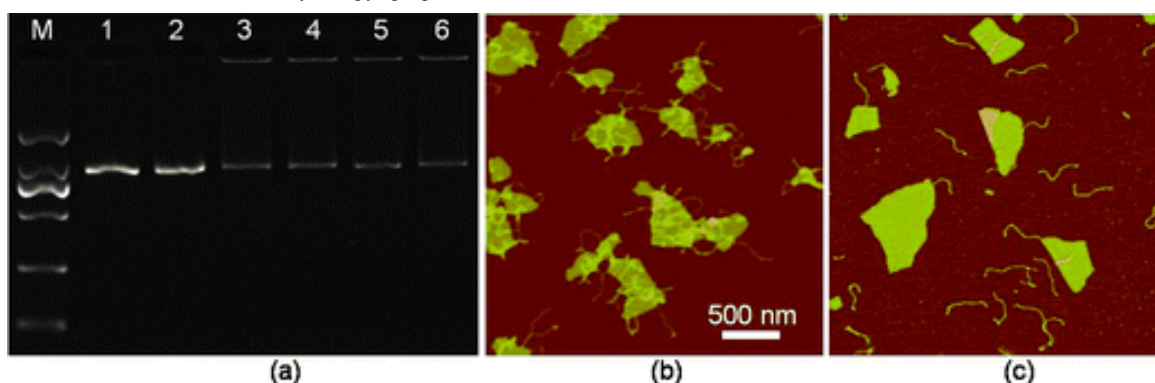


**Fig. 2** (a) An image of agarose gel electrophoresis of dsDNA and mixtures of dsDNA-GO in various buffer conditions. Lane 1: dsDNA only; lanes 2-6: mixture of dsDNA and GO ( $0.1 \text{ mg mL}^{-1}$ ) in water (Lane 2), or aqueous solutions of  $2.5 \text{ mM MgCl}_2$  (lane 3),  $5 \text{ mM CaCl}_2$  (lane 4),  $250 \text{ mM NaCl}$  (lane 5),  $50 \text{ mM KCl}$  (lane 6), respectively. (b and c) AFM images of the mixture of dsDNA and GO ( $0.15 \text{ mg mL}^{-1}$ ) prepared with DNase I reaction buffer (b), and with a pure water solution (c). Copyright permission from ref. 16.

applied to detection of protein using fluorescein-labeled aptamer-GO complex [21].

Since GO has a high affinity to ssDNA, it has been used as promising sequential delivery vehicle [22], gene-protecting [16], and transfection agent [23]. Y. Zhang et al. have investigated the  $\pi$ - $\pi$  interaction between dsDNA and GO in buffer with different metal ions. The result illustrated that the double-strands DNA (dsDNA) can be absorbed onto the GO and forms large complexes in buffers containing appropriated metal ions that prevent the degradation by dsDNA enzymes, as shown in Fig. 2 [16].

In the presence of certain metal ions (salts), such as  $\text{MgCl}_2$ ,  $\text{CaCl}_2$ , the divalent cations have a higher capability for enhancing the dsDNA molecule adsorption on GO than the monovalent cations like  $\text{K}^+$ ,  $\text{Na}^+$ . The mechanism might be speculated that GO and dsDNA tend to form complexes when metal ions neutralize the electrostatic repulsion between them [16].

It is intriguing that the GO nanosheets combing with copper ions could scissor DNA molecules. We have demonstrated that the scission of DNA by the GO/ $\text{Cu}^{2+}$  system is critically dependent on the concentrations of GO and  $\text{Cu}^{2+}$  and their ratio [17].

A possible mechanism is that GO with chelated  $\text{Cu}^{2+}$  are delivered to major groove and interacted with the electron donor groups of bases, as shown in Fig. 3. Therefore, DNA molecules were unwound and scissored

eventually [17].

Due to the abound surface oxygen-containing groups and huge surface area, GO and chemically reduced GO have been considered as ideal matrices for immobilizing enzyme and other macromolecule which could be used as biosensor [20]. Our group have investigated enzyme immobilization on CRGO with different reduction extents using horseradish peroxidase (HRP) and oxalate oxidase (OxOx) as model enzymes [20]. We found that the enzyme molecules could probably be loaded onto CRGO through hydrophobic interaction that may preserve the activity of the enzyme.

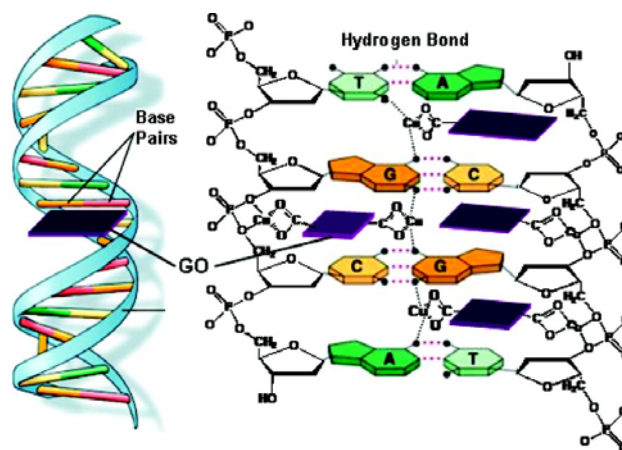


**Fig. 3** Proposed DNA cleavage mechanism by the GO/ $\text{Cu}^{2+}$  system. Copyright permission from ref. 17.

### 3. Applications for cell imaging

Owing to the unique optic-electronic properties (e.g. photoluminescence (PL)), J. Wang group has explored the conjugation of graphene (reduced graphene oxide, RGO) with quantum dots (QDs). The BSA capped QDs are grafted onto RGO. RGO were coated with polyethylenimine(PEI)/poly(sodium4-styrenesulfonate) (PSS) through electrostatic enhanced layer-by-layer assembly. [24]. Fig. 4 shows the TEM images of these complexes. The graphene-QDs emits strong luminescence with low cytotoxic effect on Hela cells as shown in Fig. 5. It is proved that graphene-QDs composites might provide a potential for non-invasive optical in vitro imaging [24]. Huang et al utilized PEG to prevent GO-induced quenching of conjugated fluorescein [25]. Thus the fluorescein-PEG-GO conjugate exhibited excellent pH-tunable fluorescent properties.

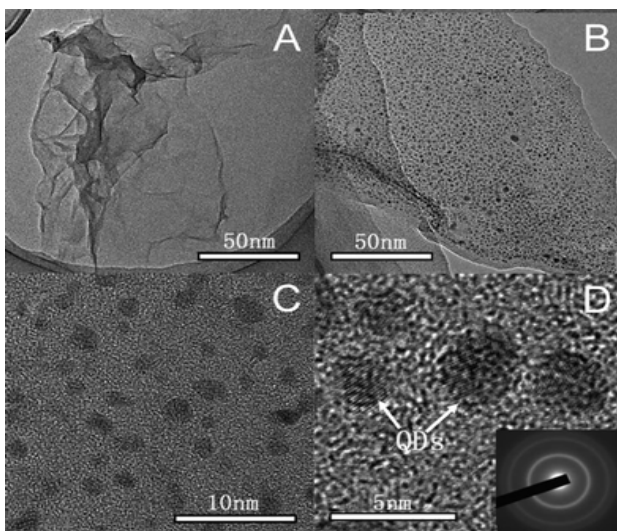


**Fig. 4** TEM images of (A) GO, (B-D) graphene-QDs. TEM images of CdTe QDs crystals on graphene sheets are observed in (C) and (D). The inset in (D) is the SAED patterns recorded from the CdTe QDs crystals on the RGO sheets. Copyright permission from ref. 24.

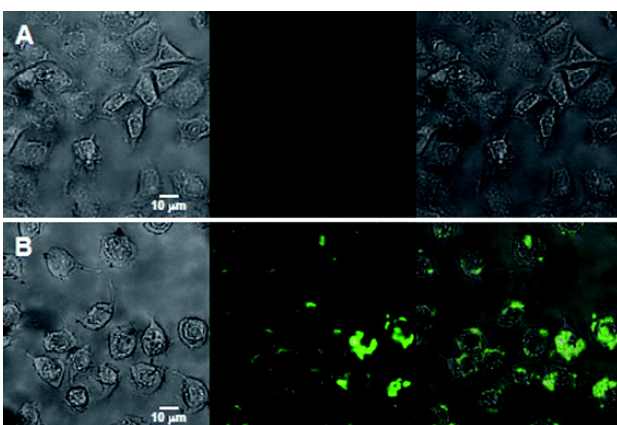


**Fig. 5** Images of Hela cells (A) without interacting with any nanoparticles, (B) directly labeled by  $60 \mu\text{g mL}^{-1}$  of graphene-QDs for 2 h. In the two panels, the left columns represent the bright-field images, the center columns represent the fluorescent images, and the right columns are the merged images of the left and center columns. Copyright permission from ref. 24.

Recently, more researches are focusing on graphene and GO with smaller lateral dimensions which were called as graphene quantum dots (GQDs). The GQDs could be synthesized through density gradient ultracentrifugal rate separation [15,27] and bottom-up fabrication [28]. The intrinsic photoluminescence of GQDs is caused by quantum confinement and edge effect [26,29,30]. Additionally, it has been demonstrated that the isolated polyaromatic structures and passivated surface defects also contribute to the fluorescence of GQDs [26,31], similar to other carbon-based fluorescent nanomaterials like the carbon dots. Therefore these GQDs with good biocompatibility possess the potential as fluorescence probe. For example, B. Yang et al have synthesized GQDs of 5.3 nm in diameter by solvothermal method, as shown in Fig. 6 [26]. They also showed that after incubation with cells, fluorescence of GQDs could be observed in dark field, as shown in Fig. 7. This is due to the unique

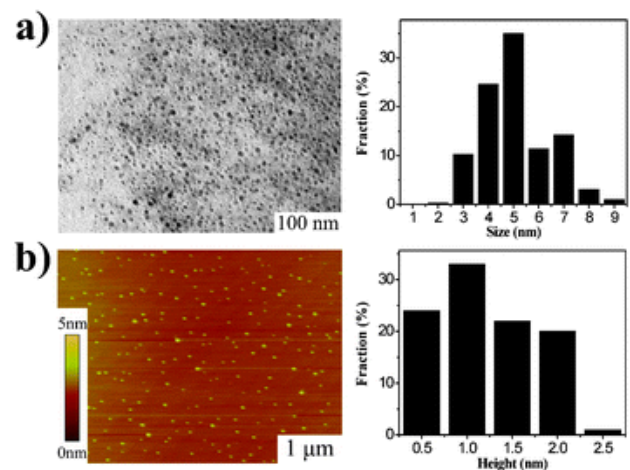


**Fig. 6** Morphology of GQDs. (a) TEM image of the GQDs (average size 5.3 nm) and their size distributions. (b) AFM image of the GQDs and their height distributions. Copyright permission from ref. 26.

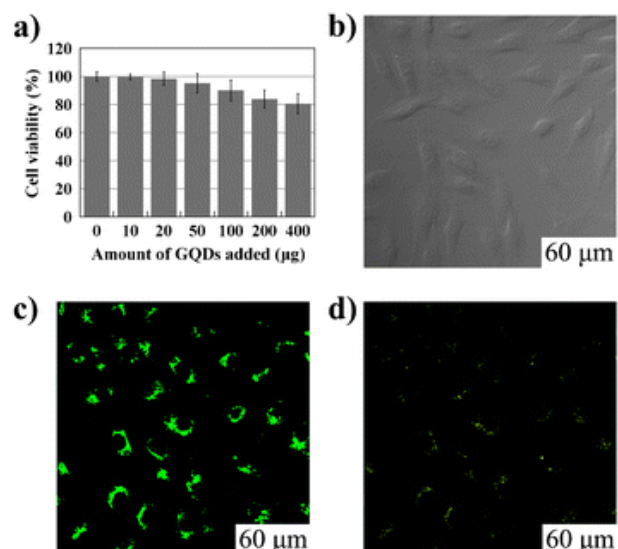


**Fig. 7** Cellular toxicity and cellular imaging of GQDs. (a) Effect of GQDs on MG-63 cells viability. (b), (c) and (d) are washed cells imaged under bright field, 405 nm, 488 nm excitations, respectively. Copyright permission from ref. 26.

http://nanobe.org

behavior of wavelength-dependent excitation of PL, that when excitation wavelengths are 405nm and 488nm, QDs exhibit green and green-yellow color, respectively [26].

H. Dai's group has synthesized nano-graphene oxide (NGO) and explored its biological applications [15]. An amine-terminated, branched PEG was used to functionalize GO, making PEGylated nano-graphene (NGO-PEG) be highly stable in physiological solutions. In near-infrared (NIR) region, live cells with little auto-fluorescence could be stained by QDs clearly. The process of NGO-PEG with Rituxan selectively binding to Raji-B cell lymphoma is illustrated in Fig. 8 (a). The process of selectively binding between NGO-PEG with Rituxan (B-cell specific antibody, or so-called anti CD-20) and Raji-B cell lymphoma is illustrated in Fig. 8 (a). After incubation with NGO-PEG-Rituxan conjugate, positive RajiB-cells exhibit bright green color in dark field, while Rituxan maintained its ability to specifically target B-cells [15].

#### 4. Applications for cancer therapy

In most cases, the aromatic drug molecules show poor water solubility, such as doxorubicin and Paclitaxel, but they might be loaded onto GO effectively through  $\pi$ - $\pi$  stacking. As delivery vehicle, GO could also deliver gene and SiRNA to enhance their efficacies.

Squaraine, a class of dyes which are known to exhibit efficient photodynamic therapeutic application, bears the positive charge, interacts with GO, but the PL could be quenched accordingly. After addition of BSA to the Squaraine-GO composite, the fluorescence intensity raises as much as 80-fold because of the improved dye delivery

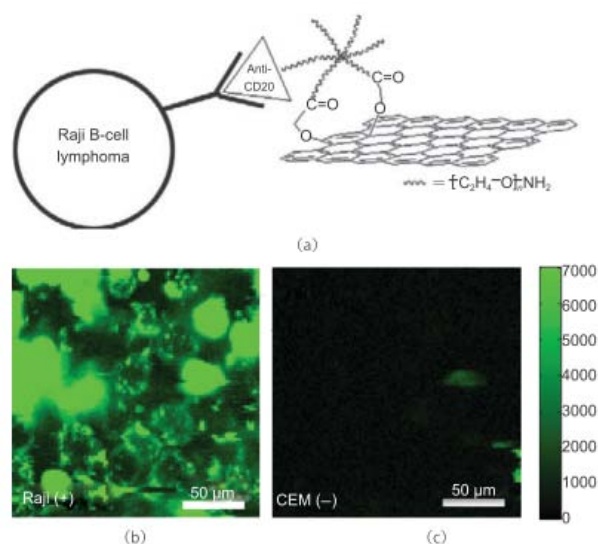


**Fig. 8** Nano-graphene for targeted NIR imaging of live cells. (a) A schematic drawing illustrating the selective binding and cellular imaging of NGO-PEG conjugated with anti-CD20 antibody, Rituxan. (b) NIR fluorescence image of CD20 positive RajiB-cells treated with the NGO-PEG-Rituxan conjugate. The scale bar shows the intensity of total NIR emission (in the range 1100-2200 nm). Images are false-colored green. (c) NIR fluorescence image of CD20 negative CEM T-Cells treated with NGO-PEG-Rituxan conjugate. Copyright permission from ref. 15.

by GO. It proves that GO could serve as a drug carrier [32].

Actually, NGO-PEG/DOX complexes have been utilized for cancer therapy in H. Dai's group [15]. In their work, the relative cell viability decreases more dramatically than that treated by free DOX.

As shown in Fig. 9, the PEGylated NGO was labeled with a NIR fluorescent dye Cy7 to study the *in vivo* behaviors of NGO. After intravenously injection of NGS-PEG-Cy7 into Balb/c mice (with 4T1 murine breast cancer) and nude mice (with KB human epidermoid carcinoma or U87MG human glioblastoma), enrichment of NGS-PEG-Cy7 was observed in sites of tumors with high fluorescence, as shown in Fig. 10. The UV-vis-NIR spectrum showed that the NGO-PEG with a size range of 10-50 nm could absorb NIR light highly. The high NIR absorption of NGO-PEG was successfully utilized for *in vivo* photothermal ablation of tumors (Fig. 11) [33].

Early in 2011, Z. Liu et al. demonstrated that the Chlorin e6 loaded on PEGylated GO could be delivered into cells due to the efficient cell entry of GO-PEG. Moreover, they show that the combination of the NIR light-triggered photothermal effect of graphene and the photodynamic treatment using Ce6 delivered by GO-PEG could enhance the PDT efficacy remarkably [34].

In addition, the chitosan-functionalized GO and PEI-grafted GO were also used as a nanocarrier for drug and gene[23], and SiRNA [22] deliveries to achieve enhanced therapy.

#### 5. Toxicity of graphene and graphene oxide

Although many potential biological and medical

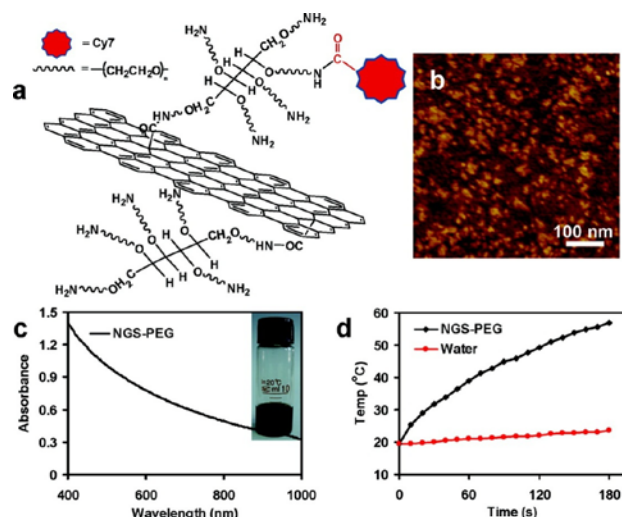


**Fig. 9** NGS functionalized with PEG. (a) A scheme of a NGS with PEG functionalization and labeled by Cy7. (b) An AFM image of NGS-PEG. (c) A UV-vis-NIR spectrum of a NGS-PEG solution at the concentration of 0.05 mg mL<sup>-1</sup>. NGS has high optical absorption from UV to NIR regions. Inset: a photo of a NGS-PEG solution at the concentration of 0.5 mg mL<sup>-1</sup>. (d) Temperature change curves of the NGS-PEG solution and the water exposed to the 808 nm laser at a power density of 2 W cm<sup>-2</sup>. Rapid raise of temperature was noted for the NGS-PEG solution, in marked contrast to the water temperature which showed little change during the laser irradiation. Copyright permission from ref. 33.

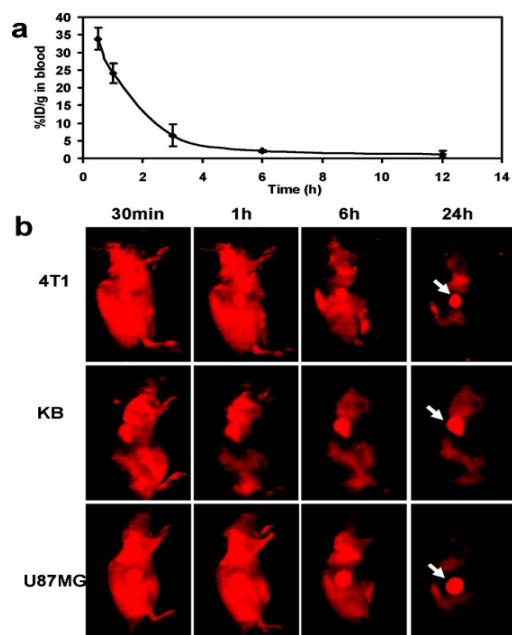


**Fig. 10** *In vivo* behaviors of NGS-PEG-Cy7. (a) The blood circulation curve of NGS-PEG-Cy7 determined by measuring Cy7 fluorescence in the blood at different time points post injection. The unit was a percentage of injected dose per gram tissue (% ID/g). Error bars were based on triplicated samples. (b) Spectrally unmixed *in vivo* fluorescence images of 4T1 tumor bearing Balb/c mice, KB, and U87MG tumor bearing nude mice at different time points post injection of NGS-PEG-Cy7. Mouse autofluorescence was removed by spectral unmixing in the above images. High tumor uptake of NGS-PEG-Cy7 was observed for all of the three tumor models. Hairs on Balb/c mice were removed before fluorescence imaging. Copyright permission from ref. 33.

applications of graphene and its derivatives have been explored, their toxicities are remained to be debated. So far, there were many researches focusing on cytotoxicity of graphene and GO. For example, H. Wang et al have investigated GO-induced cytotoxicity *in vitro* through cell morphology, cell viability, cell mortality, membrane integrity and reactive oxygen species(ROS) level. Their results suggest that GO can not enter A549 cells and has no obvious toxicity. However, GO can cause a loss of cell viability at high concentration [35].

Graphene with poor water solubility could cause some cells apoptosis and death. Y. Zhang et al. have showed that graphene can increase the activation of caspase [3], which releases of lactate dehydrogenase and activates generation of ROS, in neural pheochromocytoma-derived PC12 cells [10,36].

Different results also emerged. Through methythiazolydiphenyl-tetrazolium bromide (MTT) assay, C. Haynes and coworkers found that it fails to predict the toxicity of graphene oxide and graphene toxicity because of a false positive result induced by the spontaneous reduction of MTT by graphene and GO. The water-soluble tetrazolium salt (WST-8), trypan blue exclusion, and reactive oxygen species assay have also been used as alternate assessments to assay the toxicity [37].

On the other hand, for testing the *in vivo* toxicity, GO without any modification was injected into mice and

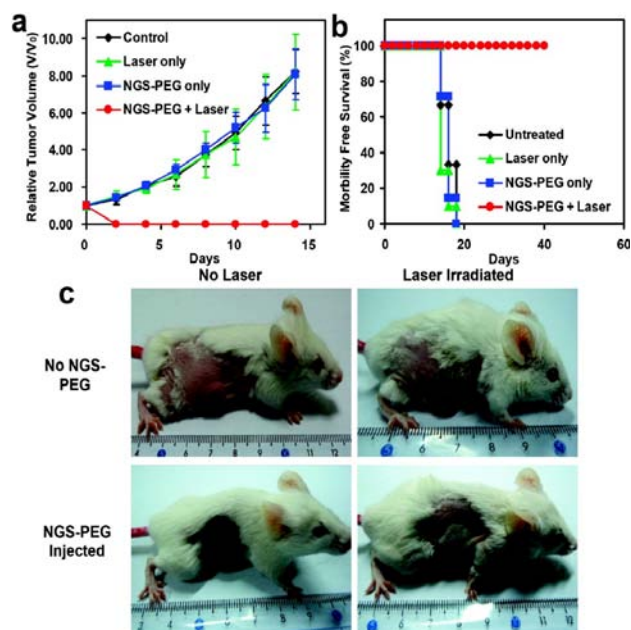


**Fig. 11** *In vivo* photothermal therapy study using intravenously injected NGS-PEG. (a) Tumor growth curves of different groups after treatment. The tumor volumes were normalized to their initial sizes. There were 6 mice in the untreated, 10 mice in the 'laser only', 7 mice in the 'NGS-PEG only', and 10 mice in the 'NGS-PEG+laser' groups. While injection of NGS-PEG by itself or laser irradiation on uninjected mice did not affect tumor growth, tumors in the treated group were completely eliminated after NGS-PEG injection and the followed NIR laser irradiation. (b) Survival curves of mice bearing 4T1 tumor after various treatments indicated. NGS-PEG injected mice after photothermal therapy survived over 40 days without any single death. (c) Representative photos of tumors on mice after various treatments indicated. The laser irradiated tumor on NGS injected mouse was completely destructed. Error bars in (a) were based on standard deviations. Copyright permission from ref. 33.

dose-dependent pulmonary toxicity, accumulating in lungs, was observed after. The reason is that physiological environment caused GO agglomerate [10]. However, PEGylated-NGO mainly localized in liver and spleen [10,33].

## 6. Conclusions

Due to the  $\pi$ - $\pi$  stacking force and hydrophobic interaction, it has been demonstrated that the graphene and GO could interact with biomacromolecules, such as DNA and enzymes, and may affect their biochemical properties. Therefore, graphene and GO could be utilized for enzymes immobilization and DNA detection. On the other hand, graphene-based composites and graphene quantum dots with tiny lateral dimension possess photoluminescence property. It has also been proved that they are promising candidates for biomolecules detection, cell imaging and cancer treatment. If the cytotoxicity and biodegradation could be addressed, the application of graphene and graphene-based nanomaterials in practical use would be unlimited. On the other hand, whether graphene and GO would bring hazardous effect on cells is still in intensive debate. If the concern of cytotoxicity could be addressed, the application of graphene and graphene-based nanomaterials in practical use would be unlimited.

http://nanobe.org

## Acknowledgements

This work was supported by the NSFC (20906055), National "973 Program" (No.2010CB933900) and the State key laboratory of bioreactor engineering (No. 2060204).

## References

- 1 K.S. Novoselov, A.K. Geim, S.V. Morozov, D. Jiang, Y. Zhang, S.V. Dubonos, I.V. Grigorieva, A.A. Firsov, Electric field effect in atomically thin carbon films. *Science* 2004; 306: 666-9.
- 2 Z.S. Wu, W. Ren, L. Gao, J. Zhao, Z. Chen, B. Liu, D. Tang, B. Yu, C. Jiang, H.M. Cheng, Synthesis of graphene sheets with high electrical conductivity and good thermal stability by hydrogen arc discharge exfoliation. *ACS Nano* 2009; 3: 411-7.
- 3 A. Reina, X. Jia, J. Ho, D. Nezich, H. Son; V. Bulovic, M.S. Dresselhaus, J. Kong, Large area, few-layer graphene films on arbitrary substrates by chemical vapor deposition. *Nano Lett.* 2009; 9: 30-35.
- 4 P.W. Sutter, J.I. Flege, E.A. Sutter, Epitaxial graphene on ruthenium. *Nat. Mater.* 2008; 7: 406-11.
- 5 D. Li, M.B. Müller, S. Gilje, R.B. Kaner, G.G. Wallace, Processable aqueous dispersions of graphene nanosheets. *Nat. Nanotechnol.* 2008; 3: 101-105.
- 6 V.C. Tung, M.J. Allen, Y. Yang, R.B. Kaner, High-throughput solution processing of large-scale graphene. *Nat. Nanotechnol.* 2009; 4: 25-29.
- 7 J. Zhang, H. Yang, G. Shen, P. Cheng, J. Zhang, S. Guo, Reduction of graphene oxide vial-ascorbic acid. *Chem. Comm.* 2010; 46: 1112.
- 8 T. Kuila, S. Bose, P. Khanra, A.K. Mishra, N.H. Kim, J.H. Lee, A green approach for the reduction of graphene oxide by wild carrot root. *Carbon* 2012; 50: 914-921.
- 9 A.K. Geim, Graphene: status and prospects. *Science* 2009; 324: 1530-1534.
- 10 L. Feng, Z. Liu, Graphene in biomedicine: opportunities and challenges. *Nanomedicine (Lond)* 2011; 6: 317-324.
- 11 A.K. Geim, K.S. Novoselov, The rise of graphene. *Nat. Mater.* 2007; 6: 183-191.
- 12 S. Guo, S. Dong, Graphene and its derivative-based sensing materials for analytical devices. *J. Mater. Chem.* 2011; 21: 18503.
- 13 S. Yang, X. Feng, S. Ivanovici, K. Mullen, Fabrication of graphene-encapsulated oxide nanoparticles: towards high-performance anode materials for lithium storage. *Angew. Chem. Int. Ed. Engl.* 2010; 49: 8408-8411.
- 14 Z. Liu, J.T. Robinson, X. Sun, H. Dai, PEGylated nanographene oxide for delivery of water-insoluble cancer drugs. *J Am Chem Soc.* 2008; 130: 10876-7.
- 15 X. Sun, Z. Liu, K. Welsler, J.T. Robinson, A. Goodwin, S. Zaric, H. Dai, Nano-graphene oxide for cellular imaging and drug delivery. *Nano Res.* 2008; 1: 203-212.
- 16 H. Lei, L. Mi, X. Zhou, J. Chen, J. Hu, S. Guo, Y. Zhang, Adsorption of double-stranded DNA to graphene oxide preventing enzymatic digestion. *Nanoscale* 2011; 3: 3888.
- 17 H. Ren, C. Wang, J. Zhang, X. Zhou, D. Xu, J. Zheng, S. Guo, DNA cleavage system of nanosized graphene oxide sheets and copper ions. *ACS Nano* 2010; 4: 7169-74.
- 18 M. Wu, R. Kempaiah, J.J. Huang, V. Maheshwari, J. Liu, Adsorption and Desorption of DNA on Graphene Oxide Studied by Fluorescently Labeled Oligonucleotides. *Langmuir* 2011; 27: 2731-2738.
- 19 H. Bao, Y. Pan, Y. Ping, N.G. Sahoo, T. Wu, L. Li, J. Li, L.H. Gan, Chitosan-functionalized graphene oxide as a nanocarrier for drug and gene delivery. *Small* 2011; 7: 1569-1578.
- 20 Y. Zhang, J. Zhang, X. Huang, X. Zhou, H. Wu, S. Guo, Assembly of graphene oxide-enzyme conjugates through hydrophobic interaction. *Small* 2012; 8: 154-159.
- 21 C.H. Lu, H.H. Yang, C.L. Zhu, X. Chen, G.N. Chen, A Graphene platform for sensing biomolecules. *Angew. Chem. Int. Ed.* 2009; 48: 4785-4787.
- 22 L. Zhang, Z. Lu, Q. Zhao, J. Huang, H. Shen, Z. Zhang, Enhanced chemotherapy efficacy by sequential delivery of siRNA and anticancer drugs using PEI-grafted graphene oxide. *Small* 2011; 7: 460-464.
- 23 L. Feng, S. Zhang, Z. Liu, Graphene based gene transfection. *Nanoscale* 2011; 3: 1252.
- 24 M.L. Chen, J.W. Liu, B. Hu, J.H. Wang, Conjugation of quantum dots with graphene for fluorescence imaging of live cells. *Analyst* 2011; 136: 4277-83.
- 25 C. Peng, W. Hu, Y. Zhou, C. Fan, Q. Huang, Intracellular imaging with a graphene-based fluorescent probe. *Small* 2010; 6: 1686-1692.
- 26 S. Zhu, J. Zhang, C. Qiao, S. Tang, Y. Li, W. Yuan, B. Li, L. Tian, F. Liu, R. Hu, H. Gao, H. Wei, H. Zhang, H. Sun, B. Yang, Strongly green-photoluminescent graphene quantum dots for bioimaging applications. *Chem. Comm.* 2011; 47: 6858.
- 27 X. Sun, D. Luo, J. Liu, D.G. Evans, Monodisperse chemically modified graphene obtained by density gradient ultracentrifugal rate separation. *ACS Nano* 2010; 4: 3381-3389.
- 28 R. Liu, D. Wu, X. Feng, K. Mullen, Bottom-up fabrication of photoluminescent graphene quantum dots with uniform morphology. *J. Am. Chem. Soc.* 2011; 133: 15221-15223.
- 29 L.A. Ponomarenko, F. Schedin, M.I. Katsnelson, R. Yang, E.W. Hill, K.S. Novoselov, A.K. Geim, Chaotic Dirac billiard in graphene quantum dots. *Science* 2008; 320: 356-358.
- 30 J. Peng, W. Gao, B.K. Gupta, Z. Liu, R. Romero-Aburto, L. Ge, L. Song, L.B. Alemany, X. Zhan, G. Gao, S.A. Vithayathil, B.A. Kaiparettu, A.A. Marti, T. Hayashi, J.J. Zhu, P.M. Ajayan, Graphene quantum dots derived from carbon fibers. *Nano Lett.* 2012; 120106121847009.
- 31 J. Lu, J.X. Yang, J. Wang, A. Lim, S. Wang, K.P. Loh, One-pot synthesis of fluorescent carbon nanoribbons, nanoparticles, and graphene by the exfoliation of graphite in ionic liquids. *ACS Nano* 2009; 3: 2367-2375.
- 32 Y. Xu, A. Malkovskiy, Y. Pang, A graphene binding-promoted fluorescence enhancement for bovine serum albumin recognition. *Chem. Comm.* 2011; 47: 6662-6664.
- 33 K. Yang, S. Zhang, G. Zhang, X. Sun, S.T. Lee, Z. Liu, Graphene in mice: ultrahigh in vivo tumor uptake and efficient photothermal therapy. *Nano Lett.* 2010; 10: 3318-3323.
- 34 B. Tian, C. Wang, S. Zhang, L. Feng, Z. Liu, Photothermally enhanced photodynamic therapy delivered by nano-graphene oxide. *ACS Nano* 2011; 5: 7000-7009.
- 35 Y. Chang, S.T. Yang, J.H. Liu, E. Dong, Y. Wang, A. Cao, Y. Liu, H. Wang, In vitro toxicity evaluation of graphene oxide on A549 cells. *Toxicol. Lett.* 2011; 200: 201-210.
- 36 Y. Zhang, S.F. Ali, E. Dervishi, Y. Xu, Z. Li, D. Casciano, A.S. Biris, Cytotoxicity effects of graphene and single-wall carbon nanotubes in neural pheochromocytoma-derived PC12 cells. *ACS Nano* 2010; 4: 3181-3186.
- 37 K.H. Liao, Y.S. Lin, C.W. Macosko, C.L. Haynes, Cytotoxicity of graphene oxide and graphene in human erythrocytes and skin fibroblasts. *ACS appl. mater. inter.* 2011; 3: 2607-2615.

**Copyright:**(c) 2012 C.Y. Wu et al. This is an open-access article distributed under the terms of the Creative Commons Attribution License, which permits unrestricted use, distribution, and reproduction in any medium, provided the original author and source are credited.